Materials Chemistry Horizons RESEARCH

Inhibiting NF-κB Activation and Reversing Multidrug Resistance via Directly Targeting the DNA-Binding Loop of P50 by Small Molecules

Marzieh Nodehi [a,b,*], Roya Behazin [c,*], Ali Ebrahimi [d], Ebrahim Negaresh [d] and Mehdi Baghayeri [b,e]

[a] Department of Chemistry, Faculty of Science, Kosar University of Bojnord, P.O. Box: 9415615458, Bojnord, Iran
[b] Core of Advance Photo-electro materials, Faculty of Science, Hakim Sabzevari University, P. O. Box 9617976487, Sabzevar, Iran
[c] Research and Development Unit, Fakhar Industrial Group, Lotus Paint and Glaze Company, Rafsanjan, Iran
[d] Department of Chemistry, University of Sistan and Baluchestan, P.O. Box 98135-674, Zahedan, Iran
[e] Department of Chemistry, Faculty of Science, Hakim Sabzevari University, P. O. Box 9617976487, Sabzevar, Iran

***Corresponding author**: marziehnodehi@yahoo.com, m.nodehi@kub.ac.ir (M. Nodehi); behazin.roya@gmail.com (R. Behazin)

Mater. Chem. Horizons, 2025, 4(1), 77-90 10.22128/mch.2026.3317.1072 OPEN ACCESS

ABSTRACT

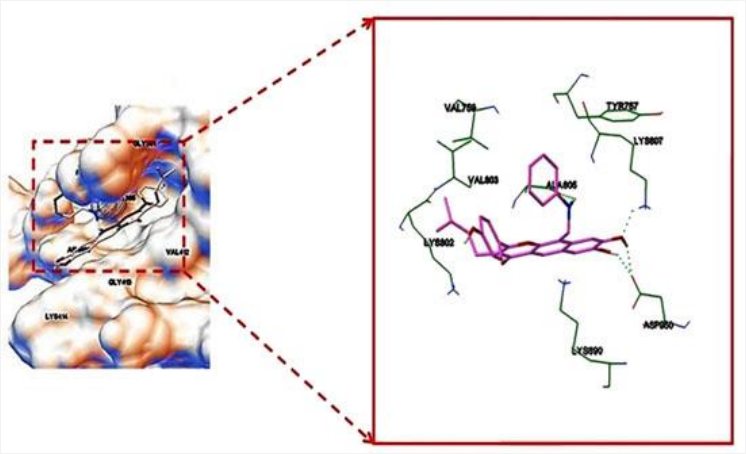

Uncontrolled nuclear factor-κB (NF-κB) pathway activation is directly involved in cancer development, inflammation, and multidrug resistance, yet potent direct inhibitors remain limited. Herein, we employed a fragment-based design strategy to develop structurally optimized chromone analogs by combining fragments derived from natural NF-κB inhibitors. Unlike previous studies that mainly focused on indirect inhibition pathways, our strategy specifically targeted the DNA-binding loop of the p50 subunit, a region essential for transcriptional regulation. Optimized geometries (B3LYP/6-31+G(d)) and fragment-based ligand variants were manually constructed, followed by automated docking into NF-κB p50 using AutoDock 4.2. Binding energies calculated for residues 356–368 identified several promising candidates. Docking studies demonstrated that some designed molecules exhibited stronger binding affinity (up to −11.13 kcal.mol^{-1}, K_i = 6.9 nM) than known reference inhibitors. Importantly, these compounds selectively inhibited NF-κB while sparing PI3K activity, thereby minimizing potential off-target effects. Furthermore, the fragment-based designed compounds showed favorable interactions with P-glycoprotein, suggesting their potential to reverse multidrug resistance. These findings introduce a rationally designed family of small molecules with dual potential for direct NF-κB inhibition and modulation of multidrug resistance.

Keywords: Natural product-inspired design, NF-κB inhibitors, P-glycoprotein, Multidrug resistance, PI3K selectivity

1. Introduction

The nuclear factor-κB (NF-κB) is a transcription factor which plays critical roles in immune and inflammatory responses that regulates the expression of a large number of genes related to cytokine production and cell survival [1, 2]. The incorrect regulation of the NF-κB proteins that belongs to Rel family, including p50/p105 (NF-κB1), p52/p100 (NF-κB1), RelA (p65), RelB and c-Rel links to development and progression of cancer, inflammatory, and autoimmune diseases. However, numerous inhibitors have been identified to suppress the NF-κB activation by which they block this pathway [3-5]. An approach for treatment of inflammation is inhibiting pro-inflammatory mediator production as is done in using inhibitors of the NF-κB activation [6].

Inhibition of the NF-κB activation can be performed directly or indirectly. The indirect and classical pathway of NF-κB activation depends on phosphorylation, ubiquitination, and degradation of kappa B (IκB) proteins, which suppresses NF-κB translocated to the nucleus and inactivate the expression of NF-κB target genes [7, 8]. Several researches tried to inhibit the degradation of the IκB proteins that can be used to modulate aberrant NF-κB signaling,

Received: May 08, 2026
Received in revised: May 29, 2026
Accepted: June 11, 2026

using small molecules such as cryptocaryone analogues [9, 10]. In contrast, a variety of inhibitors directly interact with active site of one or more NF-κB family proteins that is an effective method to prevent their function [11, 12]. The previous study has shown that the direct inhibition of the NF-κB activity in breast tumor cell lines, induce apoptosis and enhance the sensitivity of cancer cells [13, 14].

A research program on the discovery of new drug in global pharmaceutical industries showed that the structural scaffolds based on natural products can be potential agents for inhibiting a variety of targets in treatment of many diseases [15, 16]. For example, flavonoids, coumarins and chromones occur in plant exhibited a wide spectrum of useful properties such as anti-inflammatory, antibacterial, antitumor, anti-HIV, antioxidant and antiallergic [17-20]. Because of the vital role of NF-κB in cancer and various chronic diseases, numerous efforts have been performed to identify the natural products with the activity against the NF-κB pathway [21]. Many of these natural products contain heterocyclic rings that can capture active site of NF-κB by providing H-bonding and electrostatic interactions [22]. The structures of chromones that are oxygen-containing heterocyclic compounds, provide important new leads in drugs discoveries [23, 24]. Several chromone derivatives, such as 2-morpholin-4-yl-8-phenyl-chromone (LY294002) and its analogues, such as TGX-102 and TGX-286 were proposed as selective phosphatidylinositol-3-kinase (PI3K) inhibitors, where LY294002 can also inhibit the NF-κB protein [25, 26].

Xanthohumol (XN) is a prenylated flavonoid that obtained from hops has been introduced as a natural NF-κB inhibitor; it demonstrated antiproliferative, proapoptotic and antiangiogenic effects in several tumor cell lines [27, 28]. Another natural inhibitor of this protein is caffeic acid phenethyl ester (CAPE) that exists in the honeybee propolis and has anti-inflammatory, anticarcinogenic, and antioxidant activities [29-31]. Both of them can inhibit the drug efflux transporter P-glycoprotein and the reverse multidrug resistance that are effective in the cancer chemotherapy [32, 33].

The present study aimed to identify new potential candidates for direct NF-κB inhibition by targeting the DNA-binding loop involved in κB-site recognition. To achieve this goal, structural fragments derived from natural NF-κB inhibitors were combined to generate novel small molecules with enhanced inhibitory potential. In addition, the designed compounds were expected to inhibit P-glycoprotein and thereby contribute to reversing multidrug resistance.

2. Methods

The geometry optimizations were carried out at the B3LYP/6-31+G(d) level of theory using the GAUSSIAN09 program package [34]. Changing the molecular side chains, as well as scaffolds during the generation and the optimization stages is an effective method to discover new drug-like compounds [35, 36]. Fragments library were obtained from reference molecules that are related to the target, including LY294002, TGX-286, TGX-102, XN and CAPE and provided a fragment library (see **Figure 1**). It includes three types of fragments, i.e. ring (scaffold), linker and side-chain which follow several connection rules that introduced by Kawai et al. [37]. The rules are involved three allowable connections (ring−ring, ring−linker and ring−side chain connection) and three unallowable connections (linker−linker, side chain−side chain and linker−side chain connection). The designed compounds were manually constructed based on fragment combinations, and the docking simulations were subsequently carried out automatically using by AutoDock 4.2 [38]. The crystal structure of p50/p65 heterodimer of NF-κB bound to κB site of DNA obtained from Protein Data Bank. The DNA molecules and the p65 subunit removed from the protein and hydrogen atoms added to it. The active site of protein involves specific residues, such as Arg356, Tyr357, Val358, Cys359, Glu360, Gly361, Pro362, Ser363, His364, Gly365, Gly366, Leu367, and Pro368 [39]. This region corresponds to the DNA-binding loop of the p50 subunit, which plays a critical role in κB-site recognition and NF-κB transcriptional activity. Previous structural and computational studies have suggested that residues within this region can participate in ligand interactions through hydrogen bonding, electrostatic contacts, and hydrophobic interactions, making this interface a suitable target for direct inhibition of NF-κB–DNA binding. Designed molecules were docked into the p50 subunit around the region that surrounded by residues 356–368. The docking calculations were performed using AutoDock 4.2 employing the Lamarckian Genetic Algorithm (LGA). In the present study, docking simulations were carried out using a single crystal structure for each target protein (NF-κB: PDB ID 1VKX;

PI3K: PDB ID 1E7V; P-glycoprotein: PDB ID 4F4C). Ensemble docking using multiple receptor conformations was not performed. All compounds were evaluated using the same receptor structures to ensure consistency and direct comparability of docking results. The grid box was centered on the DNA-binding loop region of the p50 subunit (residues 356–368) with dimensions adjusted to fully cover the active site cavity. For each ligand, 100 GA runs were carried out using a population size of 150 individuals and a maximum number of 2.5×10^6 energy evaluations. All rotatable bonds of ligands were treated as flexible, whereas the protein receptor was kept rigid during docking simulations. Crystallographic water molecules were removed prior to docking calculations, and no explicit solvent molecules were included during the simulations. In addition, receptor flexibility and induced-fit effects were not considered, since the docking protocol was performed using a rigid protein model implemented in AutoDock 4.2.

The reported binding energies (E) correspond to the estimated free energies of binding (ΔGbinding) calculated by AutoDock 4.2 and are expressed in kcal·mol^{-1}. These values were obtained from the AutoDock scoring function, which considers intermolecular interactions, hydrogen bonding, electrostatic interactions, desolvation effects, and torsional entropy contributions.

The docking protocol was validated by re-docking the reference inhibitor into the active site of the NF-κB p50 subunit and comparing the predicted binding mode with the reported crystallographic orientation. The root-mean-square deviation (RMSD) between the experimental and re-docked conformations was used as the validation criterion. RMSD values below 2.0 Å are generally considered indicative of reliable reproduction of experimental binding poses and acceptable docking accuracy [34, 35].

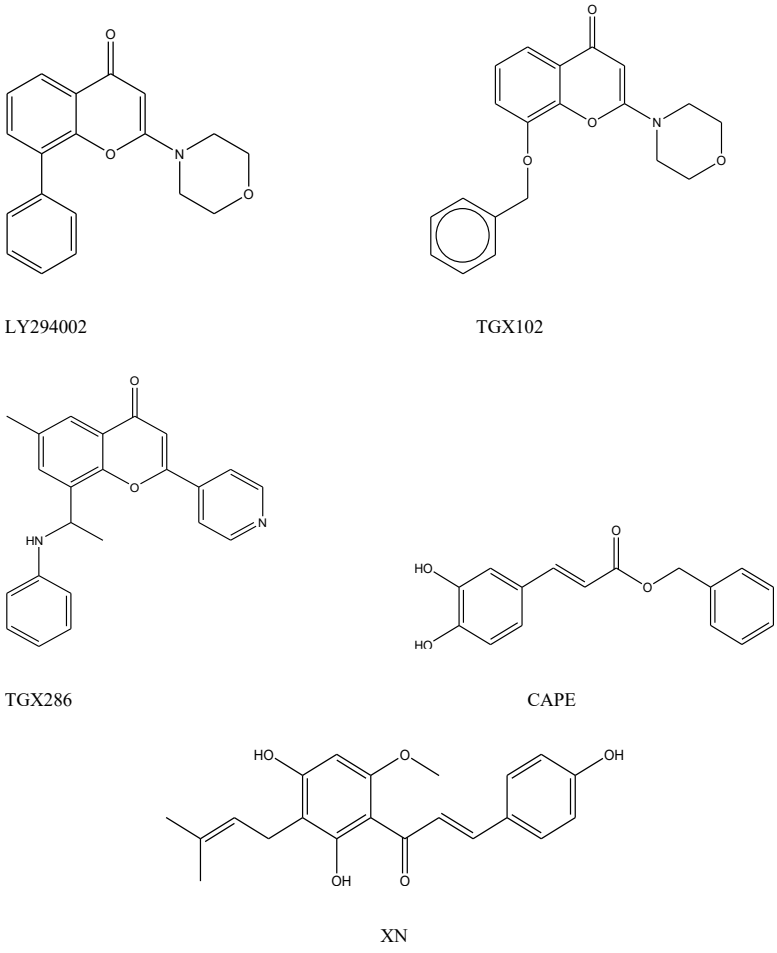

Figure 1. The chemical structures of the natural inhibitors of the NF-κB protein.

3. Results and discussion

3.1. Fragment-based design and structural derivation

The newly designed compounds were generated by strategically connecting key fragments derived from natural NF-κB inhibitors, based on rational and chemically allowable connections (**Figure 2**). This fragment-based design enabled us to capture the most pharmacologically relevant moieties of natural scaffolds while producing structurally simplified analogues with potentially enhanced bioactivity. Such a strategy provides not only a reduction in synthetic and computational complexity but also an innovative approach to achieving direct inhibition of NF-κB, which has not been sufficiently explored in previous studies [7, 40].

Notably, LY294002 and its analogues are widely recognized as specific inhibitors of phosphatidylinositol-3-kinase (PI3K), but they can also inhibit NF-κB activation independent of PI3K [41]. Since PI3K plays a crucial role in cell proliferation and survival signaling in various cells [42], selectivity against this target is a major concern in designing potent NF-κB inhibitors. Our compounds were designed with this challenge in mind, aiming to provide higher selectivity toward NF-κB while minimizing undesirable PI3K inhibition.

In addition, natural inhibitors such as XN and CAPE are known as anti-multidrug resistance agents that can prevent NF-κB activation as well as inhibit P-glycoprotein [43]. By incorporating structural features inspired from these natural scaffolds into our novel compounds, the present work offers a dual potential: direct inhibition of NF-κB and the ability to counteract P-glycoprotein–mediated multidrug resistance. This dual functionality highlights the innovative character of our design and suggests promising therapeutic implications for improving cancer chemotherapy.

Fragments of the natural inhibitors illustrated in **Figure 2**, include three types of scaffolds that the first one (A) is derived from LY294002 or its analogues. The second (B) is derived from the XN and is approximately similar to the chromones in which the pyran-4-one ring has lost a C-C bond [18, 19]. The last scaffold (C) was obtained from two fragments derived from LY294002 and CAPE. From four different linkers, two linkers were derived from TGX-102 and TGX-286, and others were derived from those by exchanging the middle atoms. In the other words, the linkers joined to benzene ring and made (R_1 as $–O-CH_2-C_6H_5$ (derived from TGX-102) that used in the structures of 1, 7 and 13 of designed molecules and $–CH(CH_3)-NH-C_6H_5$ (derived from TGX-286) that used in 6, 12 and 18 of them which are derived from TGX-102 and TGX-286 respectively. Other fragments are $–CH_2-O-C_6H_5$ (2, 8 and 14), $–NH-CH(CH_3)-C_6H_5$ (4, 10 and 16), $–NH-CH_2-C_6H_5$ (3, 9 and 15), and $–CH_2-NH-C_6H_5$ (5, 11 and 17)) where the last two cases used to determine the effect of CH_3 substituent. The R_2 side chain of designed molecules is $–C_6H_4OH$, $–NC_4H_8O$ or $–C_5H_4N$ (see **Figure 2**). The rings with the OH substituents are very common in the structures of the NF-κB inhibitors. The $–C_6H_4OH$ fragment has been derived from XN includes a six membered ring with the OH substituent, which also exists in the structures of licochalcone A, artobiloxanthone, anacardic acid, magnolol and etc. [29]. Another side chain $–NC_4H_8O$, which derived from LY294002 or TGX-102 makes H-bonding with amide backbone of CYS416 in P50 as well as Val882 residue in PI3K. The pyrimidine ring was derived from TGX-286.

The $–CH_2-CH-C(CH_3)_2$ fragment derived from XN is able to bind to the N or O atoms of amino acids because of lipophilic feature of CH_3 groups. All new designed compounds were docked in the active sites of the NF-κB and PI3K proteins to check them as suit inhibitors for NF-κB and be ineffective against PI3K. The compounds with the best results have subsequently been chosen to investigate its potential in the inhibition of P-glycoprotein; The PDB code is 1E7V for PI3K and 4F4C for P-glycoprotein.

Inhibition constant (K_i) and binding energy (E) of reference molecules in the active site of NF-κB, PI3K and P-glycoprotein are given in **Table 1**. Although TGX-286 is the best inhibitor for NF-kB where E and K_i are equal to -9.75 kcal.mol^{-1} and 70.96 nM, XN is the worst among the designed compounds when E and K_i are equal to -7.7 kcal.mol^{-1} and 2270 nM. CAPE is ineffective on PI3K with -4.12 kcal.mol^{-1} and 951670 nM for E and K_i, respectively.

Scaffolds:

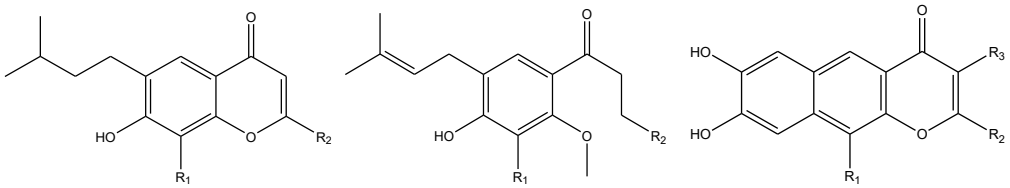

A **B** **C**

Linkers (R1):

-O-CH_2-C_6H_6 -CH_2-O-C_6H_6 -NH-CH_2-C_6H_6

-NH-CH(CH_3)-C_6H_6 -CH_2-NH-C_6H_6 -CH(CH_3)-NH-C_6H_6

Side chains (R2):

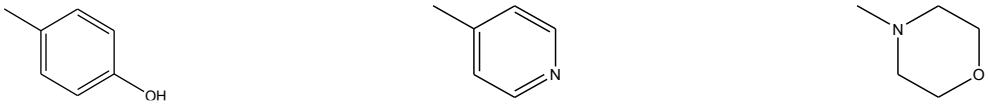

Figure 2. Fragments derived from the natural compounds and used in designing new molecules.

Table 1. The binding energy (E, in kcal.mol^{-1}) and inhibition constant (K_i, in nM) of reference molecules in the NF-κB and PI3K active sites

	NF-κB		PI3K	
	E	**K_i**	**E**	**K_i**
LY294002	-9.32	147.00	-6.83	9930
TGX-102	-8.87	314.27	-7.07	6590
TGX-286	-9.75	70.96	-7.09	6380
XN	-7.7	2270	-4.99	221780
CAPE	-8.25	890.62	-4.12	951670

3.2. Scaffold A (LY294002-derived series): potent and selective NF-κB inhibitors

Table 2 gives information about the inhibition of the NF-κB and PI3K proteins that can be used to find the most selective candidate from the first scaffold or A series where the OH and –CH_2-CH-C(CH_3)$_2$ fragments were joined to it. Most of the new structures showed greater binding affinity to the NF-κB active site compared to the reference molecules. For instance, compound A12 (R_1 = –CH(CH_3)-NH-C_6H_6 and R_2 = -C_5H_4N) exhibited binding energy (E) of -10.2 kcal·mol^{-1} and inhibition constant (K_i) of 33.13 nM. These are significantly lower than the binding energy (E = -9.75 kcal·mol^{-1}) and inhibition constant (K_i = 70.96 nM) of the reference inhibitor TGX-286. Since more negative binding energy indicates stronger molecular interactions with the protein, and inhibitory potency is indicated by the lower K_i value, the results unmistakably confirm that A12 is more strongly and effectively bound to NF-κB compared to TGX-286. The improved binding profile highlights the prospects of our designed molecules to outperform existing inhibitors against NF-κB. The best candidate for NF-κB inhibition among the designed compounds is A5 (R1 = –CH_2-NH-C_6H_6 and R_2 = –C_6H_4OH), which exhibited a binding energy (E) of –10.76 kcal.mol^{-1} and a K_i of 12.87 nM. The strong inhibitory effect of A5 can be attributed to the formation of three hydrogen bonds with key residues GLY365, VAL358, and GLY361 in the NF-κB active site. These hydrogen bonds play a critical role in stabilizing the ligand–protein complex, enhancing binding specificity, and contributing to the significantly lower Ki value compared to reference molecules. In contrast, A15 emerged as the weakest inhibitor of PI3K, with E = -6.66 kcal.mol^{-1} and K_i = 13170 nM, resulting in a very large difference in inhibitory potency

between NF-κB and PI3K (>10,000-fold). This selectivity highlights the ability of our designed molecules to target NF-κB effectively while minimizing off-target effects on PI3K, a kinase crucial for normal cell proliferation and survival signaling. These results demonstrate not only the superior binding affinity and specificity of A5 toward NF-κB, but also the innovative design strategy of the compounds, which combines structural fragments from natural inhibitors to achieve both high potency and selectivity. Compared to previously reported NF-κB inhibitors, A5 shows enhanced direct interaction with the DNA-binding loop, suggesting potential improvements in therapeutic efficiency and a promising foundation for further experimental validation. E and K_i of NF-κB are significantly changed by changing R_1 when R_2 is $–C_6H_4OH$ or $–C_5H_4N$ and it is approximately constant for PI3K. The R_1 side chain plays an important effect in the inhibition of PI3K in the presence of $–NC_4H_8O$ where the binding energies change in the range -6.66 to -8.72 kcal.mol^{-1} by changing R_1. A17 (R_1= $–CH_2$-NH-C_6H_6 and R_2= $–NC_4H_8O$) and A18 (R_1= –CH(CH_3)-NH-C_6H_6 and R_2= $–NC_4H_8O$) fit into the PI3K active site better than NF-κB in comparison with A15 (R_1= –NH-CH_2-C_6H_6 and R_2= $–NC_4H_8O$). Therefore, the strength of H-bonds between $–NC_4H_8O$ and amino acid residue can be changed by changing R_1.

In the present study, selectivity toward NF-κB was evaluated based on both the binding energy difference (ΔE) and K_i between NF-κB and PI3K. Compounds were considered strongly selective when they showed substantially lower K_i values for NF-κB, typically with at least one order of magnitude difference relative to PI3K, together with consistently more favorable binding energies toward NF-κB. Compounds exhibiting smaller differences were described as having moderate selectivity or preferential affinity toward NF-κB rather than being classified as highly selective.

Table 2. The binding energy (E, in kcal.mol^{-1}) and inhibition constant (K_i, in nM) of the A series compounds in the NF-κB and PI3K active sites.

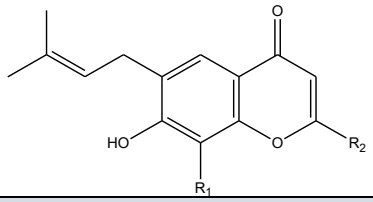

			NF-κB		PI3K	
	R_1	R_2	E	K_i	E	K_i
A1	-O-CH_2-C_6H_6	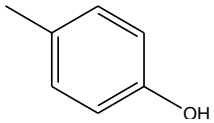	-10.54	18.85	-7.79	1960
A2	-CH_2-O-C_6H_6		-10.02	45.25	-7.39	3820
A3	-NH-CH_2-C_6H_6		-8.45	642.49	-7.95	1500
A4	-NH-CH(CH_3)-C_6H_6		-9.97	49.46	-7.28	4620
A5	-CH_2-NH-C_6H_6		-10.76	12.87	-7.37	3980
A6	-CH(CH_3)-NH-C_6H_6		-8.89	302.59	-7.85	1770
A7	-O-CH_2-C_6H_6	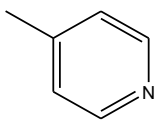	-9.95	43.99	-6.67	11150
A8	-CH_2-O-C_6H_6		-9.27	159.62	-7.51	3140
A9	-NH-CH_2-C_6H_6		-10.43	22.48	-7.2	5300
A10	-NH-CH(CH_3)-C_6H_6		-9.99	47.77	-7.31	9360
A11	-CH_2-NH-C_6H_6		-9.44	121.2	-7.71	2220
A12	-CH(CH_3)-NH-C_6H_6		-10.2	33.13	-7.52	3900

A13	-O-CH_2-C_6H_6	-8.98	261.86	-8.09	1180
A14	-CH_2-O-C_6H_6	-8.98	263.27	-7.35	4090
A15	-NH-CH_2-C_6H_6	-9.78	68.05	-6.66	13170
A16	-NH-CH(CH_3)-C_6H_6	-9.06	229.48	-7.16	5600
A17	-CH_2-NH-C_6H_6	-8.69	430.27	-8.74	394.36
A18	-CH(CH_3)-NH-C_6H_6	-8.23	924.8	-8.3	825.5

3.3. Scaffold B (Xanthohumol-Derived Series): selective inhibition with reduced PI3K affinity

As can be seen in **Table 3**, members of B series which contain second scaffold are docked in active site of NF-κB stronger than that of PI3K with the exception of B1 (R_1= –O-CH_2-C_6H_6 and R_2= –C_6H_4OH). Although these cannot inhibit the NF-κB protein as well as the A series member, they have less effect on PI3K and represent a better selectivity. As can be seen, the best result belongs to B10 (R_1= –NH-CH(CH_3)-C_6H_6 and R_2= –C_5H_4N) that E and K_i are equal to -9.42 kcal.mol^{-1} and 123.56 nM respectively, on binding to the NF-κB active site and -6.21 kcal.mol^{-1} and 28120 nM on binding to the PI3K active site. Although no strong classical hydrogen bond was observed for compound B10, the docking analysis revealed important electrostatic and weak polar interactions. In particular, electrostatic interactions were observed between the OH group and the amide backbone of SER363, while the NH group of the –NH-CH(CH3)-C6H6 side chain contributed to weak polar interactions with the C═O group of GLY365. However, B14 (R_1= –CH_2-O-C_6H_6 and R_2= –NC_4H_8O) is a compound that interacts with PI3K (E= -6.17 kcal.mol^{-1} and K_i=29810 nM) weaker in comparison with other the B series compound.

Table 3. The binding energy (E, in kcal.mol^{-1}) and inhibition constant (K_i, in nM) of the B series compounds in the NF-κB and PI3K active sites

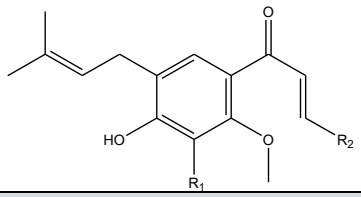

	R_1	R_2	NF-κB		PI3K	
			E	K_i	E	K_i
B1	-O-CH_2-C_6H_6		-7.64	2350	-8.14	1080
B2	-CH_2-O-C_6H_6		-8.31	804.39	-7.94	1510
B3	-NH-CH_2-C_6H_6		-8.25	902.36	-8.07	1220
B4	-NH-CH(CH_3)-C_6H_6		-8.77	373.18	-7.42	3620
B5	-CH_2-NH-C_6H_6		-8.29	833.39	-7.65	2450
B6	-CH(CH_3)-NH-C_6H_6		-8.34	764.86	-6.83	9830
B7	-O-CH_2-C_6H_6		-8.93	282.73	-6.75	11310
B8	-CH_2-O-C_6H_6		-8.54	551.88	-7.99	1380
B9	-NH-CH_2-C_6H_6		-8.61	488.32	-7.04	6850
B10	-NH-CH(CH_3)-C_6H_6		-9.42	123.56	-6.21	28120
B11	-CH_2-NH-C_6H_6		-8.54	551.53	-8.2	977.21
B12	-CH(CH_3)-NH-C_6H_6		-9.4	127.83	-7.16	5660
B13	-O-CH_2-C_6H_6		-8.47	621.54	-6.92	8510
B14	-CH_2-O-C_6H_6		-8.5	590.51	-6.17	29810
B15	-NH-CH_2-C_6H_6		-7.38	3880	-7.41	3700
B16	-NH-CH(CH_3)-C_6H_6		-8.99	255.54	-6.54	16020

B17	-CH_2-NH-C_6H_6	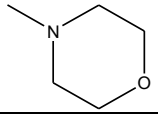	-7.69	2320	-7.39	3840
B18	-$CH(CH_3)$-NH-C_6H_6		-8.26	878.25	-6.71	12140

3.4. Scaffold C (hybrid LY294002–CAPE series): dual NF-κB and MDR inhibition

As can be seen in **Table 4**, the E and K_i values of the third scaffold (C series) introduce those as suitable candidates for the NF-κB inhibition with good selectivity. For example, the E and K_i values of C5 (R_1= –CH_2-NH-C_6H_6 and R_2= –C_6H_4OH) are equal to -11.13 kcal.mol^{-1} and 6.9 nM, so it is the best candidate, with also reasonable results for PI3K (-6.56 kcal.mol^{-1} and 14750 nM). The NH group of R_1 has a strong hydrogen bond interaction with GLY365, and also has an electrostatic interaction with PRO365, but the OH group of –C_6H_4OH and the main scaffold bind to the phenylalanine and lysine residues, respectively, by electrostatic interactions (see **Figure 3**). Eventually, these interactions make C5 a good drug-like candidate for the NF-κB inhibition, independent of PI3K with a large difference in binding energy (-4.57 kcal.mol^{-1}) and inhibition constant (>10000 nM). For compounds C2, C6, C9, C11 and C17 as candidates, the OH groups in C1 and C6-positions of scaffold are able to provide strong H-bonding and electrostatic interactions with specific residues that play important role in inhibitory effect. A hydrogen bond interaction to ILE439 and electrostatic interactions with arginine and glycine residues are observed for compound C11 (R_1= –CH_2-NH-C_6H_6 and R_2= –C_5H_4N).

The C series compounds showed promising inhibitory activity against NF-κB. To evaluate the steric effect of the substituent at the C12-position, two additional derivative series were considered. In the C′ series, the –CH_2–CH=$C(CH_3)_2$ group was replaced by H, whereas in the C″ series this group was replaced by CH_3. The corresponding binding data are presented in **Table 4**. the data in the parenthesis and bold data are related to C′ and C″ series, respectively. In spite of considerable decrease in steric hindrance in C12-position, the results do not improve on replacements. For example, E and K_i are equal to -9.56 kcal.mol^{-1} and 84.73 nM for C′5, -10.02 kcal.mol^{-1} and 45.12 nM for C″5, but are equal to -11.13 kcal.mol^{-1} and 6.9 nM for C5. As can be seen in **Table 4**, where R_2 is –NC_4H_8O or –C_5H_4N, the compounds are docked in the NF-κB active site more convenient than the compounds in which R_1 is –CH_2-CH-$C(CH_3)_2$, and the trend is not similar to those in the presence of –C_6H_4OH fragment. In the other hands, these compounds will be synthesized easier because a big group in the C12-position and the presence of a ring in the C11-position make the synthesis hard. Some of these compounds, such as C′1, C′10, C′16, C′18, C″3, C″6, C″12 and C″17 can be candidates for the NF-κB inhibition with respect to a reasonable difference between the E (and K_i) values for NF-κB and PI3K. The differences between the K_i values are higher than 10000 nM and between the E values are 3.65, 3.48, 3.47, 3.63, 3.51, 3.47, 3.66 and 3.43 kcal.mol^{-1} for the above-mentioned candidates, respectively.

Table 4. The binding energy (E, in kcal.mol^{-1}) and inhibition constant (K_i, in nM) of the C series compounds in the NF-κB and PI3K active sites.

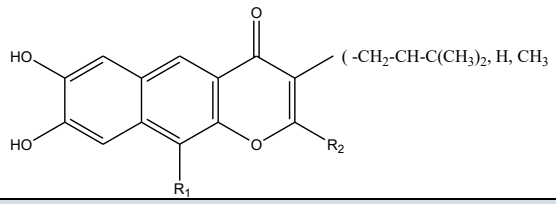

			NF-κB		PI3K	
	R_1	R_2	E	K_i	E	K_i
C1	-O-CH_2-C_6H_6	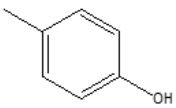	-9.56(-9.96)**-9.52**	97.74(50.02)**105.96**	-7.14(-6.31)**-6.95**	5830(23760)**13390**
C2	-CH_2-O-C_6H_6		-10.47(-9.81)**-10.04**	21.0(64.04) **43.45**	-6.96(-6.97) **-6.92**	7980(7750) **8410**
C3	-NH-CH_2-C_6H_6		-9.86(-9.86)**-9.8**	58.84(56.62) **65.95**	-7.36(-7.1) **-6.29**	4030(6200) **24710**
C4	-NH-$CH(CH_3)$-C_6H_6		-8.85(-10.06) **-10.30**	324.85(42.62) **32.89**	-7.83(-7.13) **-7.22**	1820(5900) **5130**
C5	-CH_2-NH-C_6H_6		-11.13(-9.65) **-10.02**	6.9(84.73) **45.12**	-6.56(-6.61) **-6.5**	14750(14360) **17280**
C6	-$CH(CH_3)$-NH-C_6H_6		-10.46(-9.95) **-9.57**	21.47(50.63) **96.91**	-7.11(-7.19) **-6.1**	6110(5390) **33730**

C7	-O-CH_2-C_6H_6	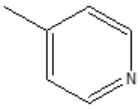	-8.3(-10.03) **-10.15**	817.84(44.11) **36.26**	-7.31(-6.84) **-7.73**	4370(9740) **2170**
C8	-CH_2-O-C_6H_6		-9.96(-9.64) **-9.65**	50.06(85.17) **84.78**	-7.04(-6.43) **-6.71**	6940(19420) **11410**
C9	-NH-CH_2-C_6H_6		-10.48(-9.88) **-10.06**	20.47(57.19) **16.68**	-7.7(-7.41) **-7.56**	2270(3730) **2890**
C10	-NH-CH(CH_3)-C_6H_6		-8.89(-10.09) **-10.34**	302.93(39.93) **26.54**	-6.94(-6.61) **-7.45**	8120(14280)**3580**
C11	-CH_2-NH-C_6H_6		-9.56(-9.44) **-9.44**	98.73(121.21)**119.95**	-6.35(-6.21) **-6.24**	22020(29700) **26640**
C12	-CH(CH_3)-NH-C_6H_6		-8.45(-9.48) **-10.1**	643.69(111.79) **39.56**	-6.5(-6.72) **-6.44**	17180(11790)**19140**
C13	-O-CH_2-C_6H_6	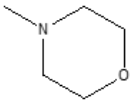	-9.43(-9.45) **-9.51**	121.63(117.97) **107.7**	-7.13(-6.49) **-6.95**	5890(17440)**8000**
C14	-CH_2-O-C_6H_6		-9.65(-9.62) **-9.42**	84.39(89.23) **124.79**	-6.75(-6.9) **-6.64**	11037(8760) **13480**
C15	-NH-CH_2-C_6H_6		-9.96(-9.67) **-9.63**	49.88(81.04) **87.69**	-7.34(-7.23) **-7.04**	4160(5000) **6900**
C16	-NH-CH(CH_3)-C_6H_6		-9.27(-10.02) **-9.96**	160.23(45.5) **49.83**	-7.14(-6.55) **-7.43**	5830(15700) **3600**
C17	-CH_2-NH-C_6H_6		-9.08(-9.7) **-9.76**	219.92(77.65) **70.45**	-6.58(-7.16) **-6.33**	15100(5670) **29970**
C18	-CH(CH_3)-NH-C_6H_6		-9.64(-10.11) **-9.55**	85.44(38.83) **99.91**	-6.89(-6.48) **-6.45**	8900(17720) **18820**

*Data in parentheses correspond to the C′ series (H at the C12-position), whereas bold values correspond to the C″ series (CH_3 at the C12-position)

3.5. Comparative docking analysis of NF-κB, PI3K, and P-glycoprotein

CAPE and XN are known to inhibit both NF-κB and P-glycoprotein, thereby exhibiting promising therapeutic effects in cancer treatment. Therefore, the inhibitory potential of the newly designed compounds against P-glycoprotein was compared with these reference molecules (**Table 5**). The results indicate that several designed compounds exhibit stronger predicted inhibitory activity toward P-glycoprotein than the reference inhibitors, suggesting their potential to reverse multidrug resistance. For example, C2 (R_1= –CH_2-O-C_6H_6 and R_2= –C_6H_4OH) and C9 (R_1= –NH-CH_2-C_6H_6 and R_2= –C_5H_4N) are the best inhibitors for the P-glycoprotein, where K_i values are equal to 350.86 and 414.03 nM, respectively. The best docked conformations of them around the active site surfaces of the NF-κB, PI3K and P-glycoprotein are shown in **Figure 3**. The main interactions are two H-bonding of the OH and C═O groups of scaffolds with the phenylalanine and glycine residues of C2 and two interactions between the OH groups of scaffolds with the glutamine residues of C9.

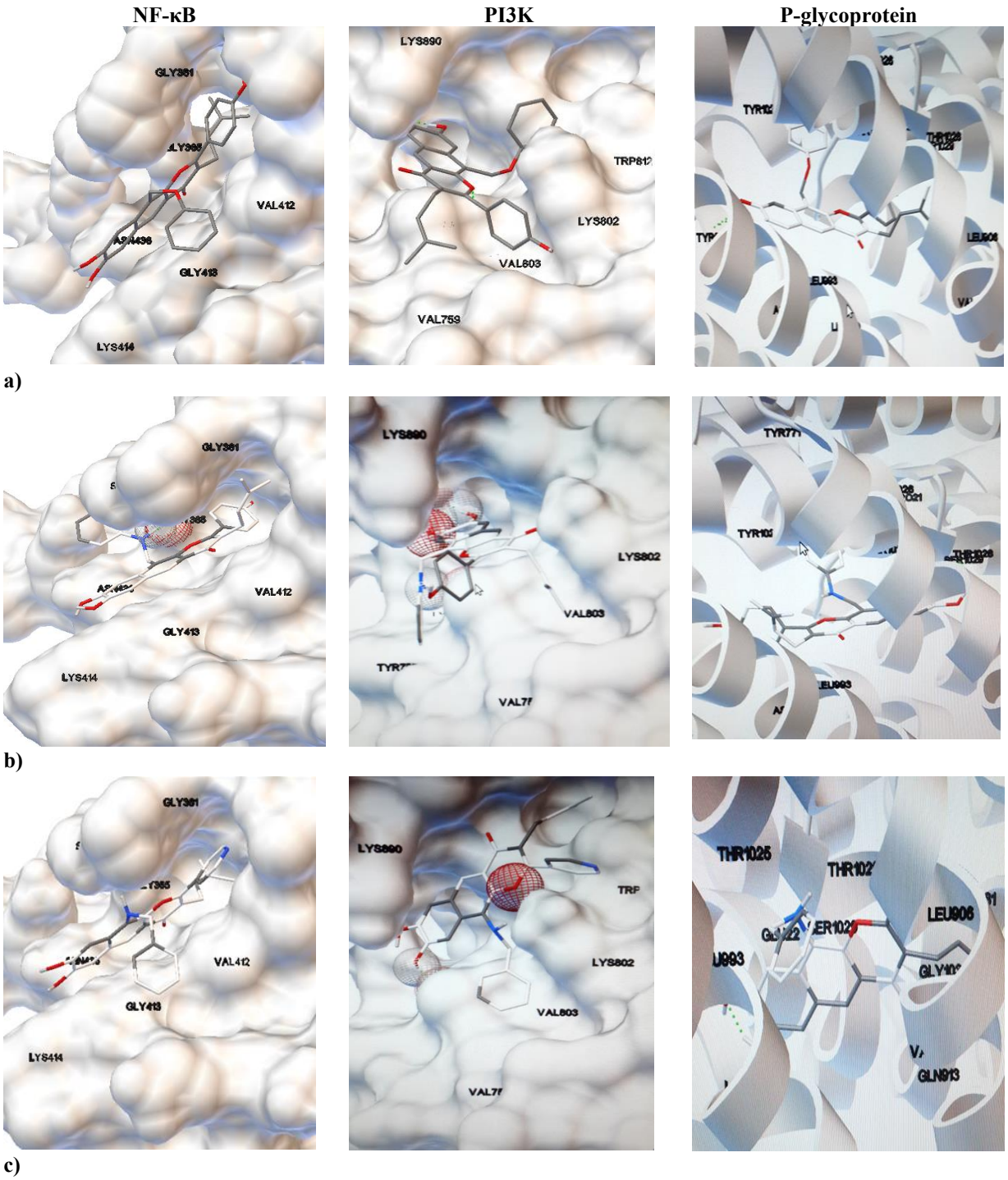

Figure 3. Docking of compounds, a) C2, b) C5 and c) C9 in the binding cavity of the NF-kB (first column), PI3K (second column) and P-glycoprotein (third column).

Table 5. The binding energy (E, in kcal.mol^{-1}) and inhibition constant (K_i, in nM) of selected compounds in the P-glycoprotein active site.

Compound	E	K_i	compound	E	K_i
A5	-7.51	3150	**C′10**	-7.92	1560
B10	-7.24	4890	**C′16**	-7.48	3300
C2	-8.81	350.86	**C′18**	-7.5	3170
C5	-8.31	811.94	**C″3**	-7.52	3090
C6	-8.29	842.09	**C″6**	-8.33	787.43
C9	-8.71	414.03	**C″12**	-7.21	5180
C11	-8.62	481.09	**C″17**	-8.17	1030
C17	-8.37	734.88	**CAPE**	-6.12	32850
C′1	-7.7	2280	**XN**	-7.41	3710

3.6. Identification of lead compounds

Lead compound selection was based on a combined evaluation of three parameters, including binding affinity toward NF-κB, selectivity relative to PI3K, and predicted inhibitory activity against P-glycoprotein. According to **Table 4**, C5 emerged as the most potent inhibitor of NF-κB, with a binding energy of –11.13 kcal.mol^{-1} and a very low inhibition constant (K_i = 6.9 nM). Importantly, its affinity toward PI3K is much weaker (E = -6.56 kcal.mol^{-1}, K_i = 14,750 nM), corresponding to more than a 2000-fold difference in selectivity. This pronounced gap highlights C5 as a highly selective NF-κB inhibitor. Moreover, as shown in **Table 5**, C5 also demonstrates reasonable inhibitory activity against P-glycoprotein (E = –8.31 kcal.mol^{-1}, K_i = 811.94 nM), which suggests that it may reduce drug efflux and consequently enhance intracellular drug accumulation. Taken together, these results indicate that C5 is not only a strong and selective NF-κB inhibitor but also a promising candidate to overcome multidrug resistance, thereby introducing it as a novel agent with dual therapeutic potential.

4. Conclusion

Direct inhibition of NF-κB activation remains an important strategy for developing selective therapeutic agents in both academic and industrial research. However, many previously reported natural NF-κB inhibitors suffer from limited selectivity toward PI3K or insufficient ability to reverse multidrug resistance. To address these limitations, we designed a series of novel compounds by integrating structural fragments derived from natural NF-κB inhibitors. Among the designed molecules, the C series exhibited the highest selectivity toward NF-κB over PI3K based on binding energy and inhibition constant analyses. Additional C′ and C″ derivatives were also evaluated to investigate steric effects at the C12-position. Furthermore, docking studies against P-glycoprotein revealed that compounds C2, C5, and C9 may possess multidrug resistance–reversing activity. Collectively, these findings highlight the effectiveness of our fragment-based design strategy for developing multifunctional NF-κB inhibitors with potential applications in cancer therapy and inflammatory disorders.

Acknowledgment

The financial support for this project from University of Sistan and Baluchestan is greatly appreciated.

Authors' contributions

Marzieh Nodehi: Corresponding author and manuscript editing. Roya Behazin: Analysis and writing of the original manuscript. Ali Ebrahimi: Supervisor and research. Ebrahim Negaresh: Research and writing of the original manuscript. Mehdi Baghayeri: Manuscript editing

Declaration of competing interest

The authors declare that they have no conflict of interest.

Funding

This paper received no funding.

Data availability

Data will be made available on request.

References

[1] F.G. Bauernfeind, G. Horvath, A. Stutz, E.S. Alnemri, K. MacDonald, D. Speert, T. Fernandes-Alnemri, J. Wu, B.G. Monks, K.A. Fitzgerald, Cellular immunology and immune regulation, J. Immunol. 183 (2009) 785-1496. **DOI**: https://doi.org/10.4049/jimmunol.0901365

[2] J. Xu, Y.-Y. Jia, S.-R. Chen, J.-T. Ye, X.-Z. Bu, Y. Hu, Y.-Z. Ma, J.-L. Guo, P.-Q. Liu, (E)-1-(4-ethoxyphenyl)-3-(4-nitrophenyl)-prop-2-en-1-one suppresses LPS-induced inflammatory response through inhibition of NF-κB signaling pathway, Int. Immunopharmacol. 15 (2013) 743-751. **DOI**: https://doi.org/10.1016/j.intimp.2013.02.018

[3] A. Csiszar, K. Smith, N. Labinskyy, Z. Orosz, A. Rivera, Z. Ungvari, Resveratrol attenuates TNF-α-induced activation of coronary arterial endothelial cells: role of NF-κB inhibition, Am. J. Physiol. Heart Circ. Physiol. 291 (2006) H1694-H1699. **DOI**: https://doi.org/10.1152/ajpheart.00360.2006

[4] J.i. Inoue, J. Gohda, T. Akiyama, K. Semba, NF-κB activation in development and progression of cancer, Cancer Sci. 98 (2007) 268-274. **DOI**: https://doi.org/10.1111/j.1349-7006.2007.00395.x

[5] M. Karin, Nuclear factor-κB in cancer development and progression, Nature 441 (2006) 431-436. **DOI**: https://doi.org/10.1038/nature04870

[6] X.-F. Wu, Z.-J. Ouyang, L.-L. Feng, G. Chen, W.-J. Guo, Y. Shen, X.-D. Wu, Y. Sun, Q. Xu, Suppression of NF-κB signaling and NLRP3 inflammasome activation in macrophages is responsible for the amelioration of experimental murine colitis by the natural compound fraxinellone, Toxicol. Appl. Pharmacol. 281 (2014) 146-156. **DOI**: https://doi.org/10.1016/j.taap.2014.09.003

[7] S.C. Gupta, C. Sundaram, S. Reuter, B.B. Aggarwal, Inhibiting NF-κB activation by small molecules as a therapeutic strategy, Biochim. Biophys. Acta Gene Regul. Mech. 1799 (2010) 775-787. **DOI**: https://doi.org/10.1016/j.bbagrm.2010.05.004

[8] S. Ghosh, M.S. Hayden, New regulators of NF-κB in inflammation, Nat. Rev. Immunol. 8 (2008) 837-848. **DOI**: https://doi.org/10.1038/nri2423

[9] D.J. Van Antwerp, I.M. Verma, Signal-induced degradation of IκBα: association with NF-κB and the PEST sequence in IκBα are not required, Mol. Cell. Biol. 16 (1996) 6037-6045. **DOI**: https://doi.org/10.1128/MCB.16.11.6037

[10] C. Jobin, A. Panja, C. Hellerbrand, Y. Iimuro, J. Didonato, D.A. Brenner, R.B. Sartor, Inhibition of proinflammatory molecule production by adenovirus-mediated expression of a nuclear factor κB super-repressor in human intestinal epithelial cells, J. Immunol. 160 (1998) 410-418. **DOI**: https://doi.org/10.4049/jimmunol.160.1.410

[11] D.C. Swinney, Y.-Z. Xu, L.E. Scarafia, I. Lee, A.Y. Mak, Q.-F. Gan, C.S. Ramesha, M.A. Mulkins, J. Dunn, O.-Y. So, A small molecule ubiquitination inhibitor blocks NF-κB-dependent cytokine expression in cells and rats, J. Biol. Chem. 277 (2002) 23573-23581. **DOI**: https://doi.org/10.1074/jbc.M200842200

[12] D. Wu, S. Tian, W. Zhu, Modulating multidrug resistance to drug-based antitumor therapies through NF-κB signaling pathway: mechanisms and perspectives, Expert Opin. Ther. Targets 27 (2023) 503-515. **DOI**: https://doi.org/10.1080/14728222.2023.2228682

[13] H. Zhou, D.M. Monack, N. Kayagaki, I. Wertz, J. Yin, B. Wolf, V.M. Dixit, Yersinia virulence factor YopJ acts as a deubiquitinase to inhibit NF-κB activation, J. Exp. Med. 202 (2005) 1327-1332. **DOI**: https://doi.org/10.1084/jem.20051194

[14] M.A. Occhiuzzi, G. Lico, G. Ioele, M. De Luca, A. Garofalo, F. Grande, Recent advances in PI3K/PKB/mTOR inhibitors as new anticancer agents, Eur. J. Med. Chem. 246 (2023) 114971. **DOI**: https://doi.org/10.1016/j.ejmech.2022.114971

[15] J.-H. Lee, T.H. Koo, B.Y. Hwang, J.J. Lee, Kaurane diterpene, kamebakaurin, inhibits NF-κB by directly targeting the DNA-binding activity of p50 and blocks the expression of antiapoptotic NF-κB target genes, J. Biol. Chem. 277 (2002) 18411-18420. **DOI**: https://doi.org/10.1074/jbc.M111304200

[16] A. Glaviano, A.S. Foo, H.Y. Lam, K.C. Yap, W. Jacot, R.H. Jones, H. Eng, M.G. Nair, P. Makvandi, B. Geoerger, PI3K/AKT/mTOR signaling transduction pathway and targeted therapies in cancer, Mol. Cancer 22 (2023) 138. **DOI**: https://doi.org/10.1186/s12943-023-01827-6
[17] K.-C. Tsai, L.-W. Teng, Y.-M. Shao, Y.-C. Chen, Y.-C. Lee, M. Li, N.-W. Hsiao, The first pharmacophore model for potent NF-κB inhibitors, Bioorg. Med. Chem. Lett. 19 (2009) 5665-5669. **DOI**: https://doi.org/10.1016/j.bmcl.2009.08.032
[18] J.K. Hexum, R. Tello-Aburto, N.B. Struntz, A.M. Harned, D.A. Harki, Bicyclic cyclohexenones as inhibitors of NF-κB signaling, ACS Med. Chem. Lett. 3 (2012) 459-464. **DOI**: https://doi.org/10.1021/ml3000302
[19] P. Bremner, M. Heinrich, Natural products as targeted modulators of the nuclear factor-κB pathway, J. Pharm. Pharmacol. 54 (2002) 453-472. **DOI**: https://doi.org/10.1211/0022357021778790
[20] F. Folmer, W.T. Harrison, J.N. Tabudravu, M. Jaspars, W. Aalbersberg, K. Feussner, A.D. Wright, M. Dicato, M. Diederich, NF-κB-inhibiting naphthopyrones from the Fijian echinoderm Comanthus parvicirrus, J. Nat. Prod. 71 (2008) 106-111. **DOI**: https://doi.org/10.1021/np070488n
[21] T. Okamoto, S. Yoshida, T. Kobayashi, S. Okabe, Inhibition of concanavalin A-induced mice hepatitis by coumarin derivatives, Jpn. J. Pharmacol. 85 (2001) 95-97. **DOI**: https://doi.org/10.1254/jjp.85.95
[22] B.H. Havsteen, The biochemistry and medical significance of the flavonoids, Pharmacol. Ther. 96 (2002) 67-202. **DOI**: https://doi.org/10.1016/S0163-7258(02)00298-X
[23] B. Ngameni, M. Touaibia, R. Patnam, A. Belkaid, P. Sonna, B.T. Ngadjui, B. Annabi, R. Roy, Inhibition of MMP-2 secretion from brain tumor cells suggests chemopreventive properties of a furanocoumarin glycoside and of chalcones isolated from the twigs of Dorstenia turbinata, Phytochemistry 67 (2006) 2573-2579. **DOI**: https://doi.org/10.1016/j.phytochem.2006.09.006
[24] A. Sajid, H. Rahman, S.V. Ambudkar, Advances in the structure, mechanism and targeting of chemoresistance-linked ABC transporters, Nat. Rev. Cancer 23 (2023) 762-779. **DOI**: https://doi.org/10.1038/s41568-023-00618-z
[25] M. Chaturvedi, B. Sung, V. Yadav, R. Kannappan, B. Aggarwal, NF-κB addiction and its role in cancer: 'one size does not fit all', Oncogene 30 (2011) 1615-1630. **DOI**: https://doi.org/10.1038/onc.2010.537
[26] M. Kawase, T. Tanaka, H. Kan, S. Tani, H. Nakashima, H. Sakagami, Biological activity of 3-formylchromones and related compounds, In Vivo 21 (2007) 829-834.
[27] A. Gaspar, M.J. Matos, J. Garrido, E. Uriarte, F. Borges, Chromone: a valid scaffold in medicinal chemistry, Chem. Rev. 114 (2014) 4960-4992. **DOI**: https://doi.org/10.1021/cr400540p
[28] R.M. Gunn, H.C. Hailes, Insights into the PI3-K-PKB-mTOR signalling pathway from small molecules, J. Chem. Biol. 1 (2008) 49-62. **DOI**: https://doi.org/10.1007/s12154-008-0008-7
[29] V.R. Yadav, S. Prasad, B. Sung, B.B. Aggarwal, The role of chalcones in suppression of NF-κB-mediated inflammation and cancer, Int. Immunopharmacol. 11 (2011) 295-309. **DOI**: https://doi.org/10.1016/j.intimp.2010.12.010
[30] M. Liu, P.E. Hansen, G. Wang, L. Qiu, J. Dong, H. Yin, Z. Qian, M. Yang, J. Miao, Pharmacological profile of xanthohumol, a prenylated flavonoid from hops (Humulus lupulus), Molecules 20 (2015) 754-779. **DOI**: https://doi.org/10.3390/molecules20010754
[31] M. Demestre, S. Messerli, N. Celli, M. Shahhossini, L. Kluwe, V. Mautner, H. Maruta, CAPE (caffeic acid phenethyl ester)-based propolis extract (Bio 30) suppresses the growth of human neurofibromatosis (NF) tumor xenografts in mice, Phytother. Res. 23 (2009) 226-230. **DOI**: https://doi.org/10.1002/ptr.2593
[32] K. Natarajan, S. Singh, T.R. Burke Jr, D. Grunberger, B.B. Aggarwal, Caffeic acid phenethyl ester is a potent and specific inhibitor of activation of nuclear transcription factor NF-kappa B, Proc. Natl. Acad. Sci. USA 93 (1996) 9090-9095. **DOI**: https://doi.org/10.1073/pnas.93.17.9090
[33] T. Nabekura, T. Hiroi, T. Kawasaki, Y. Uwai, Effects of natural nuclear factor-kappa B inhibitors on anticancer drug efflux transporter human P-glycoprotein, Biomed. Pharmacother. 70 (2015) 140-145. **DOI**: https://doi.org/10.1016/j.biopha.2015.01.005
[34] M. Frisch, Gaussian 09, Revision D.01, Gaussian, Inc., Wallingford CT, 2009. https://gaussian.com/
[35] C. Bruyère, S. Madonna, G. Van Goietsenoven, V. Mathieu, J. Dessolin, J.-L. Kraus, F. Lefranc, R. Kiss, JLK1486, a Bis 8-hydroxyquinoline-substituted benzylamine, displays cytostatic effects in experimental gliomas through MyT1 and STAT1 activation and, to a lesser extent, PPARγ activation, Transl. Oncol. 4 (2011) 126-127. **DOI**: https://doi.org/10.1593/tlo.10241
36] T. Schlick, S. Portillo-Ledesma, C.G. Myers, L. Beljak, J. Chen, S. Dakhel, D. Darling, S. Ghosh, J. Hall, M. Jan, Biomolecular modeling and simulation: a prospering multidisciplinary field, Annu. Rev. Biophys. 50 (2021) 267-301. **DOI**: https://doi.org/10.1146/annurev-biophys-091720-084000

[37] K. Kawai, N. Nagata, Y. Takahashi, De novo design of drug-like molecules by a fragment-based molecular evolutionary approach, J. Chem. Inf. Model. 54 (2014) 49-56.
DOI: https://doi.org/10.1021/ci400483a
[38] G.M. Morris, R. Huey, W. Lindstrom, M.F. Sanner, R.K. Belew, D.S. Goodsell, A.J. Olson, AutoDock4 and AutoDockTools4: automated docking with selective receptor flexibility, J. Comput. Chem. 30 (2009) 2785-2791. **DOI**: https://doi.org/10.1002/jcc.21256
[39] V. Pande, R.K. Sharma, J.-I. Inoue, M. Otsuka, M.J. Ramos, A molecular modeling study of inhibitors of nuclear factor kappa-B (p50)-DNA binding, J. Comput. Aided Mol. Des. 17 (2003) 825-836. **DOI**: https://doi.org/10.1023/B:JCAM.0000021393.27333.10
[40] T. Kobayashi, A. Yoshimori, K. Kino, R. Komori, H. Miyazawa, S.-i. Tanuma, A new small molecule that directly inhibits the DNA binding of NF-κB, Bioorg. Med. Chem. 17 (2009) 5293-5297.
DOI: https://doi.org/10.1016/j.bmc.2009.05.031
[41] Y.H. Kim, K.-H. Choi, J.-W. Park, T.K. Kwon, LY294002 inhibits LPS-induced NO production through a inhibition of NF-κB activation: independent mechanism of phosphatidylinositol 3-kinase, Immunol. Lett. 99 (2005) 45-50. **DOI**: https://doi.org/10.1016/j.imlet.2004.12.010
[42] N.N. Ahmed, H.L. Grimes, A. Bellacosa, T.O. Chan, P.N. Tsichlis, Transduction of interleukin-2 antiapoptotic and proliferative signals via Akt protein kinase, Proc. Natl. Acad. Sci. USA 94 (1997) 3627-3632. **DOI**: https://doi.org/10.1073/pnas.94.8.3627
[43] H. Dudek, S.R. Datta, T.F. Franke, M.J. Birnbaum, R. Yao, G.M. Cooper, R.A. Segal, D.R. Kaplan, M.E. Greenberg, Regulation of neuronal survival by the serine-threonine protein kinase Akt, Science 275 (1997) 661-665. **DOI**: https://doi.org/10.1126/science.275.5300.661